AD-A136 718 EFFECT OF ELECTROMAGNETIC STIRRING ON WELD POOLS(U) 1/1
DAVID W TAYLOR NAVAL SHIP RESEARCH AND DEVELOPMENT
CENTER ANN.. R DENALE ET AL. OCT 83 DTNSRDC/SME-83/65
UNCLASSIFIED F/G 11/6 NL

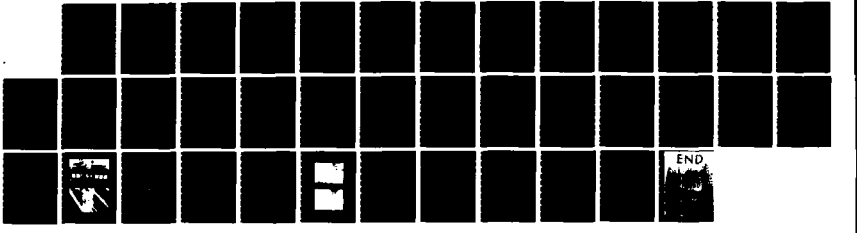

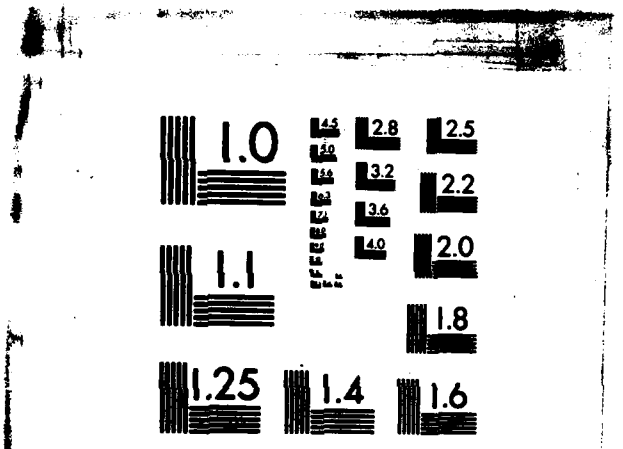

MICROCOPY RESOLUTION TEST CHART
NATIONAL BUREAU OF STANDARDS-1963-A

DAVID W. TAYLOR NAVAL SHIP RESEARCH AND DEVELOPMENT CENTER

Bethesda, Maryland 20084

EFFECT OF ELECTROMAGNETIC STIRRING ON WELD POOLS

by

R. DeNale and W. E. Lukens

APPROVED FOR PUBLIC RELEASE: DISTRIBUTION UNLIMITED

SHIP MATERIALS ENGINEERING DEPARTMENT

RESEARCH AND DEVELOPMENT REPORT

OCTOBER 1983

DTNSRDC SME-83/65

MAJOR DTNSRDC ORGANIZATIONAL COMPONENTS

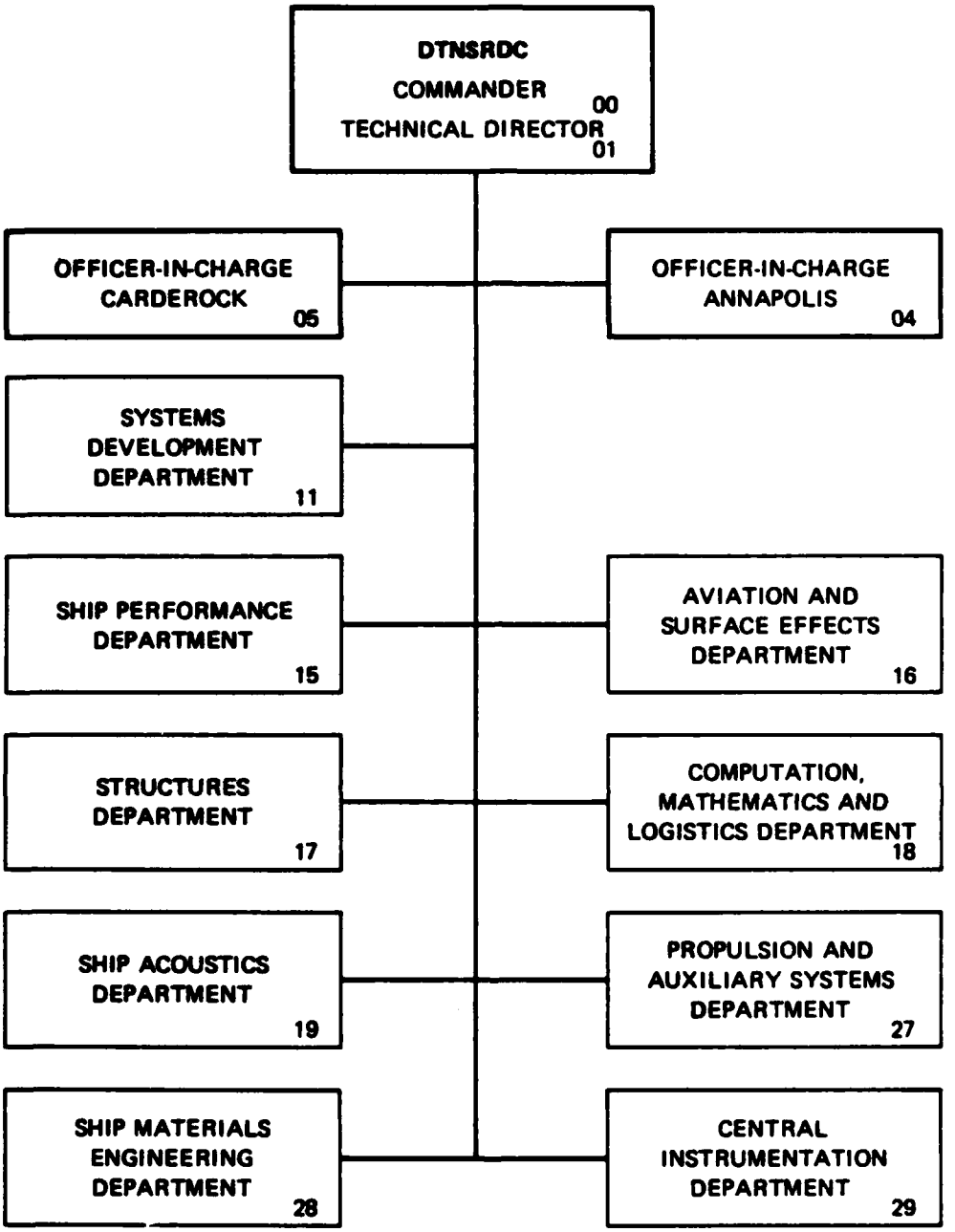

UNCLASSIFIED

SECURITY CLASSIFICATION OF THIS PAGE (When Data Entered)

REPORT DOCUMENTATION PAGE	READ INSTRUCTIONS BEFORE COMPLETING FORM
1. REPORT NUMBER: DTNSRDC/SME-83/65	2. GOVT ACCESSION NO.: AD-A136718
3. RECIPIENT'S CATALOG NUMBER	
4. TITLE (and Subtitle): EFFECT OF ELECTROMAGNETIC STIRRING ON WELD POOLS	5. TYPE OF REPORT & PERIOD COVERED: Research & Development
	6. PERFORMING ORG. REPORT NUMBER
7. AUTHOR(s): R. DeNale and W. E. Lukens	8. CONTRACT OR GRANT NUMBER(s)
9. PERFORMING ORGANIZATION NAME AND ADDRESS: David Taylor Naval Ship R&D Center, Bethesda, MD 20084	10. PROGRAM ELEMENT, PROJECT, TASK AREA & WORK UNIT NUMBERS: Element No. 61153N, Projects-RR022-01-01, RR022-11-0B, Work Unit 2822-143,2822-144
11. CONTROLLING OFFICE NAME AND ADDRESS: Office of Naval Research, Arlington, VA 22217	12. REPORT DATE: October 1983
	13. NUMBER OF PAGES: 34
14. MONITORING AGENCY NAME & ADDRESS(if different from Controlling Office)	15. SECURITY CLASS. (of this report): UNCLASSIFIED
	15a. DECLASSIFICATION/DOWNGRADING SCHEDULE

16. DISTRIBUTION STATEMENT (of this Report)

Approved for Public Release: Distribution Unlimited

17. DISTRIBUTION STATEMENT (of the abstract entered in Block 20, if different from Report)

18. SUPPLEMENTARY NOTES

19. KEY WORDS (Continue on reverse side if necessary and identify by block number)

GTAW
Electromagnetic Agitation
Titanium
Thermal Gradient

20. ABSTRACT (Continue on reverse side if necessary and identify by block number)

Autogenous gas tungsten arc welds were made perpendicular to the rolling direction on a single heat of Ti-6Al-4V alloy. A commercial electromagnetic arc control system producing a transverse magnetic field that enabled the arc to be rotated at frequencies ranging from 0 to 35 Hz. Control welds were made without arc rotation. Two series of welds were made with the rotating arc, one at a welding speed of 1.7 mm/s and the second at a welding speed of 3.4 mm/s. The frequency of arc rotation was varied from 1 to 35 Hz while all other welding variables were maintained constant.

DD FORM 1 JAN 73 1473 EDITION OF 1 NOV 65 IS OBSOLETE
S/N 0102-LF-014-6601

UNCLASSIFIED

SECURITY CLASSIFICATION OF THIS PAGE (When Data Entered)

Block 20 Continued

Metallographic examination was performed transverse and parallel to the longitudinal axis of the weld to determine the effect of arc rotation on the size of the columnar grains associated with titanium welding, the depth of penetration, and the width of the weld bead. In general, increasing the frequency of arc rotation over the range studied had no effect on the area, major axis or minor axis of the columnar grains for either of the welding speeds employed. For the series which employed a welding speed of 1.7 mm/s the depth of penetration decreased initially and then increased to the depth of the contol series. Conversely, the weld bead width increased initially with the introduction of arc rotation. With a welding speed of 3.4 mm/s, arc rotation had a detrimental effect on the weld bead contour.

In addition, temperature measurements were performed on a control series of autogenous gas tungsten arc welds and a series of gas tungsten arc welds produced while rotating the arc at 10 Hz. The thermal profiles of the welds were measured by dragging a sheathed and grounded tungsten - rhenium thermocouple at a fixed distance behind the centerline of the tungsten electrode for approximately 15 seconds, releasing the thermocouple by breaking a fusible link attached between the torch and a carriage on which the thermocouple was positioned, and recording temperature as a function of distance after release. Additional welds were produced in which the thermocouple was dragged from a control (unstirred) weld into a stirred weld pool. It was found that at the position studied there was minimal superheat in the weld pool. Additionally, the weld pool temperature decreased at a fixed distance behind the centerline of the tungsten electrode when stirring was employed. Futhermore, arc rotation caused a decrease in the thermal gradient associated with the semi-solid zone.

Finally, calculations comparing the equilibrium liquidus temperature with the actual weld pool temperatures indicated that cellular or dendritic as opposed to planar growth were probable; however, the size of the supercooled region was so small that grain refinement due to the postulated mechanisms (dendrite tip fragmentation, etc.) would not be expected.

TABLE OF CONTENTS

LIST OF FIGURES

LIST OF TABLES

LIST OF ABBREVIATIONS

A	Ampere	Hz	Hertz
°C	Degree Celsius	in.	Inch
cm	Centimeter	ℓ	Liters
cfh	Cubic feet per hour	min.	Minute
DCEN	Direct Current Electrode Negative		
°F	Degree Fahrenheit	mm	Millimeter
G	Gauss	T	Tesla
GTAW	Gas Tungsten Arc Welding	V	Voltage

CONVERSION FACTORS

1 ℓ/min = 2.12 cfh

$$°C = \frac{5\,(°F - 32)}{9}$$

1 cm = 0.394 in.

1 mm = 0.039 in.

1 T = 10^4 G

ABSTRACT

Weld metal grain refinement has been the objective of many investigations. Various methods to refine grains have been used and include ultrasonic and mechanical vibration, inoculation, forced convective cooling, and electromagnetic agitation. Electromagnetic agitation has several advantages over other methods of grain refinement in that it is directly applicable to a wide range of existing alloys, readily adaptable to the welding torch, and does not require mechanical coupling to the weldment. Numerous investigations have employed electromagnetic agitation to produce rotation of the weld pool to achieve weld metal grain refinement. A majority of these investigations used a superimposed magnetic field that was coaxial with the welding arc. Several proposed mechanisms for grain refinement due to electromagnetic agitation have included: dendrite tip fragmentation, weld pool temperature equilibration, accelerated side wall growth, and periodic melting and reorientation of secondary dendrite branches. Some investigators have reported the effects on the weld metal microstructure of a superimposed magnetic field that is transverse to the welding arc. The objective of this program is to define the mechanism of grain refinement due to electromagnetic agitation by understanding the mode of solidification, the fluid flow at the liquid-solid interface, and the thermal gradients in the semi-solid region. The work reported herein used a commercial electromagnetic arc control system producing a transverse magnetic field that enabled the arc to be rotated at frequencies ranging from 0 to 35 Hz.

Autogenous gas tungsten arc welds were made perpendicular to the rolling direction on a single heat of Ti-6Al-4V alloy. Control welds were made without arc rotation. Two series of welds were made with the rotating arc, one at a welding speed of 1.7 mm/s and the second at a welding speed of 3.4 mm/s. The frequency of arc rotation was varied from 1 to 35 Hz while all other welding variables were maintained constant.

Metallographic examination was performed transverse and parallel to the longitudinal axis of the weld to determine the effect of arc rotation on the size of the columnar grains associated with titanium welding, the depth of penetration, and the width of the weld bead. In general, increasing the frequency of arc rotation over the range studied had no effect on the area, major axis or minor axis of the columnar grains for either of the welding speeds employed. For the series which employed a welding speed of 1.7 mm/s the depth of penetration

decreased initially and then increased to the depth of the control series. Conversely, the weld bead width increased initially with the introduction of arc rotation and decreased with increasing frequency of rotation. With a welding speed of 3.4 mm/s, arc rotation had a detrimental effect on the weld bead contour.

In addition, temperature measurements were performed on a control series of autogenous gas tungsten arc welds and a series of gas tungsten arc welds produced while rotating the arc at 10 Hz. The thermal profiles of the welds were measured by dragging a sheathed and grounded tungsten - rhenium thermocouple at a fixed distance behind the centerline of the tungsten electrode for approximately 15 seconds, releasing the thermocouple by breaking a fusible link attached between the torch and a carriage on which the thermocouple was positioned, and recording temperature as a function of distance after release. Additional welds were produced in which the thermocouple was dragged from a control (unstirred) weld into a stirred weld pool. It was found that at the position studied there was minimal superheat in the weld pool. Additionally, the weld pool temperature decreased at a fixed distance behind the centerline of the tungsten electrode when stirring was employed. Futhermore, arc rotation caused a decrease in the thermal gradient associated with the semi-solid zone.

Finally, calculations comparing the equilibrium liquidus temperature with the actual weld pool temperatures indicated that cellular or dendritic as opposed to planar growth were probable; however, the size of the supercooled region was so small that grain refinement due to the postulated mechanisms (dendrite tip fragmentation, etc.) would not be expected.

ADMINISTRATIVE INFORMATION

This investigation was conducted under Work Units 2822-143 and 2822-144 titled, "Mechanism of Grain Refinement," funded as Research Projects RR022-01-01 and RR014-11-0B, Program Element 61153N, sponsored by Dr. B. A. MacDonald (ONR 431). The Work Unit leader was Dr. W. E. Lukens of the Welding Branch (DTNSRDC 2815). The technical agent was Dr. O. P. Arora (DTNSRDC 2811). The effort was supervised by Mr. C. A. Zanis, Head, Welding Branch (DTNSRDC 2815). This report satisfies milestones 2822-143-10 and 2822-144-10.

INTRODUCTION

BACKGROUND

Weld metal grain refinement has been the objective of many investigations. Various methods to refine grains have been used and include mechanical vibration,[1] inoculation,[2,3] forced convective cooling[4,5] and electromagnetic agitation.[1,6-13] Electromagnetic agitation has successfully been used for grain refinement in castings and has several advantages over other methods of weld metal grain refinement in that it is readily adaptable to the welding torch, does not require mechanical coupling to the weldment, and is directly applicable to a wide range of alloys.

Various investigations[1,12-13] have reported that electromagnetic agitation suppresses the columnar growth of the weld metal in unalloyed titanium and Ti-6Al-4V (reduction in grain size was approximately 10 to 1); however, grain refinement of Ti-13V-11Cr-3Al did not occur. Similarly, other investigators[9,10] have reported that alternating external magnetic fields cause extensive grain refinement in some aluminum alloys while in other aluminum alloys alternating external magnetic fields had little or no effect on grain refinement.

There are conflicting views reported as to the mechanism involved in weld metal grain refinement due to electromagnetic agitation. Brown[1] suggests that electromagnetic stirring produces a relative shear force between the liquid and solid at the solidifying interface which can cause fragmentation of dendrites, provide an increased number of atoms to critical sized nuclei, or mix higher melting composition solute back to the supercooled region and thus enhance nucleation. Chernysh[6] states that electromagnetic stirring equilizes the mean temperature of the molten pool in the semi-solid region relative to the temperature along the axis of welding and accelerates

solidification of the pool by a factor of 2-3. In a later investigation Chernysh[7] proposes that the primary structure of weld metal is refined due to higher solidification rates combined with periodic melting of crystals when electromagnetic stirring is employed. Abralov [8] proposes that electomagnetic agitation refines the primary structure grain size by periodically melting the bases of secondary dendrite branches, separating the branches away from the main arm, and allowing a new grain to grow without an additional nucleus.

Examination of these and other investigations[9-13] into the cause of weld metal grain refinement due to electromagnetic agitation indicates that the important areas for study to determine the mechanism governing grain refinement include solidification, fluid dynamics, and heat transfer. The objective of this work is to define the mechanism of grain refinement due to electromagnetic agitation by understanding the mode of solidification, the fluid flow at the liquid-solid interface and the thermal gradients in the semi-solid region.

In the present investigation the use of commercial electromagnetic arc control equipment was explored as a means of refining weld metal grain size. In addition, a unique apparatus was developed to measure the thermal gradient of the semi-solid region.

SOLIDIFICATION THEORY

The fact that the liquidus and solidus of most alloys do not coincide, shown schematically in Figure 1a, indicates that the solubility of the solute, at a given temperature, is different in the solid and liquid phases. Upon freezing, this difference in solubility results in the partitioning of solute at the solid-liquid interface and, consequently, differing equilibrium

compositions in the liquid and the solid, Figure 1a. The concentrations of the solute in the solid and the liquid at the interface are C_s and C_L, respectively. The ratio of these concentrations is defined as the equilibrium distribution coefficient, k_o, that is,

$$k_o = \frac{C_s}{C_L}. \tag{1}$$

Diffusion of the solute in the solid is usually much slower than in the liquid. Assuming that equilibrium exists at the interface, ignoring diffusion in the solid, allowing diffusion as the only transport mechanism in the liquid, and considering the rate of the advancing interface, R, results in the solute distribution shown in Figure 1b. The distribution of the solute due to rejection at the advancing interface and diffusion into the liquid is represented by the curve. Since the composition of the solid equals the initial composition of the liquid, C_o, a steady state condition can exist and only in this case does the amount of solute in the enriched layer of the liquid remain constant. Thus, the concentration of the solute in the liquid at a distance, x, ahead of the interface can be expressed as follows[14]

$$C_L = C_o \left[1 + \frac{1-k_o}{k_o} \exp\left(\frac{-R}{D} x\right) \right] \tag{2}$$

where D is the diffusion coefficient of the solute in the liquid. The diffusion coefficients for liquid metals are the same within a factor of ten; 5×10^{-5} cm^2/s being a representative value.[15]

Under the conditions which prevail during solidification of the weld pool, the assumption of mixing by diffusion only is unlikely because of temperature gradients and surface tension driven flow which promote natural convection.[16] The effect of mixing on solute redistribution due to fluid motion by

convection has been reported by Wagner.[17] Wagner states that the solute moves only by diffusion through a laminar flow of fluid of thickness, d, beyond which convection controls and dictates a uniform liquid composition, C_M. This layer of laminar flow is sufficiently thick so as to include all of the diffusion zone when motion of the liquid is confined to natural convection. When motion of the liquid is more violent the boundary layer is not thick enough to accomodate the entire diffusion zone, in which case diffusion controls the motion of solute up to a point beyond which mixing predominates, see Figure 1c.

The equilibrium liquidus temperature is dependent on solute concentration according to the phase diagram, see Figure 1a. As the liquid is enriched due to rejection of solute at the solid-liquid interface, the equilibrium liquidus temperature decreases ahead of the advancing interface. The equilibrium liquidus temperature ahead of the interface is shown schematically in Figure 1d and is given [14] for a position at the interface by

$$T_e = T_o - mC_L \tag{3}$$

where m is the slope of the liquidus line $\left(dT_e/dC_L\right)$ and T_o is the equilibrium melting temperature for the pure metal. For any point, x, ahead of the interface the equilibrium liquidus temperature can be obtained by substituting equation (2) into (3) and obtaining

$$T_e = T_o - mC_o\left[1 + \frac{1-k_o}{k_o} \exp\left(\frac{-R}{D}x\right)\right]. \tag{4}$$

With the introduction of mixing, the concentration of the solute in the liquid beyond the effective diffusion zone is increased and therefore the equilibrium liquidus temperature is decreased as shown in Figure 1e.

The actual temperature at any point in the liquid is given by

$$T = T_o - \frac{mC_o}{k_o} + Gx \qquad (5)$$

where G is the thermal gradient and $T_o - \frac{mC_o}{k_o}$ is the temperature at the interface. A positive thermal gradient is normally found in the weld pool because the heat source is at the center. However, because of the decrease in equilibrium liquidus temperature at the interface, it is possible, even with a positive thermal gradient, to have a region of supercooled liquid, see Figure 1f. Therefore, the possibility of dendritic growth even in the presence of a positive thermal gradient exists.

ELECTROMAGNETIC STIRRING

Electromagnetic stirring operates on the principle of a resultant force on a current-carrying conductor due to a uniform magnetic field, B. The welding current, i, consists of the electrons in both the arc plasma and the weld pool. When the welding current is placed in a uniform magnetic field the normal components of current and magnetic flux result in a force which is perpendicular to both. By orienting the magnetic flux transverse or along the axis of the welding electrode different effects can be obtained.

When the magnetic flux is transverse to the axis of the electrode, as shown in Figure 2a, the magnetic field interacts with the vertical component of the current and results in arc deflection. Minimal interaction between B and the current in the weld pool occurs because the magnitude of B at any point is inversely proportional to the square of distance. Therefore the magnetic field is greatest at the probe tips and rapidly decreases with increasing distance. By rotating the magnetic field around the axis of the electrode the deflected arc is also rotated.

When the magnetic flux is coaxial with the electrode, as shown in Figure 2b, the magnetic field interacts with the horizontal component of the current and results in arc and liquid metal rotation.

APPARATUS

MAGNETIC FIELD GENERATOR

The Cyclomatic Arc Pattern Control system used in this study consists of a solid state control panel, Model 90A, and a water cooled probe, Model 4613A, which fits around the welding torch nozzle. This system employs a transverse magnetic field which provides magnetic control of the arc along two axes and interdependent amplitude and frequency controls. The magnetic flux generated depends on the frequency of rotation and can be varied from 0.01 to 0.06T.

THERMAL PROFILER

The equipment developed to measure the thermal gradient of the weld pool semi-solid region consists of an enclosure which provides inert gas coverage of the weld specimen, excellent visibility of the arc and weld pool, and a platform on which a thermocouple carriage is transported (Figure 3a). The thermocouple carriage holds a tantalum sheathed, grounded, tungsten - 5% rhenium: tungsten - 26% rhenium thermocouple and is maintained at a constant position behind the welding torch by means of a fusible link (Figure 3b). The thermoelectromotive force is recorded as a function of time on a chart recorder. The abscissa in units of time is converted to distance by applying a voltage to the recorder at measured intervals along the surface of the specimen.

EXPERIMENTAL PROCEDURES

Two sets of experiments were conducted. Autogenous gas tungsten arc welds were made with and without arc rotation to determine the effect of stirring frequency on grain size. Additionally, autogenous gas tungsten arc welds were made with and without electromagnetic stirring during which a thermocouple was dragged at a fixed distance from the electrode to determine the effect of stirring on thermal gradients.

In the first set of tests, two series of welds were produced at two travel speeds, 1.7 and 3.4 mm/s, while the frequency of arc rotation was varied from 0 to 35 Hz, see Table 1. All other welding variables were maintained constant. Metallographic examination was performed transverse (TS plane) and parallel (LS plane) to the longitudinal axis of the weld to determine the effect of arc rotation on the area, major axis, and minor axis of the columnar grains.

In the second set of tests, temperature measurements were performed on a control series of autogenous gas tungsten arc welds and a series of gas tungsten arc welds while rotating the arc at 10 Hz. The thermal profiles of the welds were measured by initiating an arc on the leading edge of pre-existing weld craters, establishing a weld pool and at the same time preheating the thermocouple with arc radiated heat, initiating travel which in turn immersed the thermocouple in the weld pool, dragging the thermocouple in the weld pool at a fixed distance behind the centerline of the tungsten electrode for approximately 15 seconds to establish equilibrium conditions, and releasing the thermocouple by breaking a fusible link attached between the torch and thermocouple carriage. Additional welds were produced in which the thermocouple was dragged from an unstirred weld pool into a stirred weld pool.

The thermocouple was positioned 8 mm behind the centerline of the electrode along the axis of the weld. Positions closer to the arc were attempted; however, with the welding variables employed 8 mm was the minimum distance from the electrode centerline that the thermocouple could be reliably immersed into the weld pool without melting. The depth of immersion was 2 mm and was determined by metallographic techniques. The positioning of the thermocouple is shown schematically in Figure 4.

WELDING PROCEDURES

All the weld beads were produced bead-on-plate, perpendicular to the rolling direction, in the flat position under carefully controlled and monitored conditions.

The set of welds made to determine the effect of stirring frequency on grain size employed automated GTAW equipment with a 4 mm diameter, 2% thoriated tungsten electrode ground to a 30° included angle. The welding was done with DCEN. The arc voltage was 16 V, the current was 300A, the shielding gas was argon at 19 ℓ/min, and the travel speed was either 1.7 or 3.4 mm/s.

The set of welds made while dragging a thermocouple with and without electromagnetic stirring used automated GTAW equipment with a 4mm diameter, 2% thoriated tungsten electrode ground to a 30° included angle. The welding was done using DCEN with an arc voltage of 14 V, an amperage of 300 A, argon at 19 ℓ/min as the shielding gas, a travel speed of 1.5 mm/s, and arc rotation, when employed, at 10 Hz.

TEST MATERIAL

The plate material used in all of the tests was 30 X 230 X 230 mm Ti-6Al-4V. The surfaces were degreased with acetone and rotary wire brushed prior to welding.

TABLE 1 - WELDING CONDITIONS

Weld Identification	Current A	Voltage V	Travel Speed mm/s	Frequency of Arc Rotation Hz
09023-1	300	16	1.7	0
09023-2	300	16	1.7	1.5
09023-3	300	16	1.7	4.5
09023-4	300	16	1.7	7.5
09023-5	300	16	1.7	11.5
09023-6	300	16	1.7	14.5
09023-7	300	16	1.7	20.5
09023-8	300	16	1.7	25.5
09023-9	300	16	1.7	29.5
09023-10	300	16	1.7	33.5
09023-11	300	16	1.7	35
15102-1	300	16	3.4	0
15102-2	300	16	3.4	1.5
15102-3	300	16	3.4	4.5
18102-4	300	16	3.4	7.5
18102-5	300	16	3.4	11.5
18102-6	300	16	3.4	14.5
18102-7	300	16	3.4	20.5
18102-8	300	16	3.4	25.5
18102-9	300	16	3.4	29.5
18102-10	300	16	3.4	33.5
18102-11	300	16	3.4	35

RESULTS AND DISCUSSION

EFFECT OF STIRRING ON GRAIN SIZE

The parameters of travel speed and frequency of arc rotation were varied independently. All other welding conditions were held constant during each experiment. Data taken from quantitative metallographic analysis of weld cross sections in which travel speed and frequency of arc rotation were systematically varied from one series of experiments to the other are presented in Figures 5 and 6.

The data indicate that the columnar grain size, as represented in Figure 5 by the major axis of columnar grains in transverse cross sections and shown in Figure 7 did not vary considerably as a function of frequency of rotation for either welding speed employed. Similarly, increasing the frequency of arc rotation over the range studied had no effect on the area or length of minor axis transverse to the direction of welding nor was an effect noted parallel to the welding direction.

For the series which employed a welding speed of 1.7 mm/s the depth of penetration decreased initially and then increased to the depth of the control specimens. Conversely, the weld bead width increased initially with the introduction of arc rotation and decreased with increasing frequency of rotation. For the series which employed a welding speed of 3.4 mm/s arc rotation had a detrimental effect on the weld bead contour and resulted in dimples which were evenly spaced on the weld bead surface.

EFFECT OF STIRRING ON TEMPERATURE

A typical thermocouple trace is shown in Figure 8 and consists of the following features: preheating of the thermocouple; the thermocouple enters

the weld pool; a liquid zone of minimal superheat; release of the thermocouple and initiation of a coordinate axis; a semi-solid zone with a steep thermal gradient; and the solid zone. At the position of the thermocouple in the liquid, 2 mm from the interface, temperature was uniform with or without stirring. In welds where the thermocouple was dragged from an unstirred weld pool into a stirred weld pool a decrease in temperature of approximately 40° C was observed. This decrease in temperature was observed only when the thermocouple had traversed 5 mm after the introduction of the magnetic field, which would bring the thermocouple to the position of the arc when the magnetic field was introduced. Therefore, it is believed that the decrease in temperature of the weld pool is due to the dissipation of arc heat over a larger area rather than a stirring motion of the weld pool. A stirring motion of the weld pool would affect the thermocouple reading as soon as the magnetic field was initiated.

In the semi-solid zone the unstirred and stirred specimens exhibited average temperature gradients of 99 and 83° C/mm. Although the position of the thermocouple relative to the tungsten electrode was the same for all experiments, stirring changed weld pool shape so that the position of the thermocouple relative to the solid-liquid interface was 2.8 mm in the unstirred weld pool and 2.0 mm in the stirred weld pool. Thus, it appears that the decrease in thermal gradients and absolute weld pool temperature in the stirred weld pool may be a result of the change in weld bead shape which resulted in the thermocouple being positioned closer to the solid-liquid interface.

MODE OF SOLIDIFICATION

The equilibrium liquidus temperature ahead of the solid-liquid interface for Ti-6Al was calculated using equation (4) and is shown is Figure 9. Additionally, Figure 9 combines equation (5), the equation for the theoretical temperature at any point ahead of the solid-liquid interface and the empirically derived thermal gradients, G, for the control and stirred welds. By comparing the equilbrium liquidus temperature and the actual weld pool temperature ahead of the solid-liquid interface, cellular or dendritic as opposed to planar growth would most probably occur because of supercooling; however, the maximum length of the supercooled region is so small, 0.07 mm, that grain refinement in Ti-6Al-4V due to the postulated mechanisms (dendrite tip freqmentation, etc.) would not be expected. The accuracy of the equilibrium liquidus temperature line would be improved by use of the ternary Ti-6Al-4V diagram.

ALLOY SYSTEM AND PLATE THICKNESS

The ability to refine grain size is dependent on two important factors which have not yet been discussed, alloy system and plate thickness. The importance of the alloy system has been recognized by other investigators in that a large separation of the solidus-liquidus will result in a larger semi-solid zone and dendritic growth will be encouraged. Dendritic growth is necessary for grain refinement by dendrite tip fragmentation or secondary drendrite arm separation. An understanding of the mechanism of grain refinement as it applies to the Ti-6Al-4V system will be enhanced by consideration of solidus-liquidus separation with respect to other alloy systems.

The effect of plate thickness on grain refinement has not been discussed in the literature and may play a critical role in the ability to refine grains. Thin plate, 6mm or less, approximates 2-dimensional heat flow, especially in full penetration welds. There is only a small thermal gradient in the through thickness direction. The solidification grains grow in the direction of maximum thermal gradients and will have their major axes parallel to the plate surface as shown in Figure 10a. Grains oriented in this manner may be more amenable to refinement due to periodic remelting at the interface. Thick plate heat flow occurs 3-dimensionally, and the grains have their major axis in the through thickness direction, as shown in Figure 10b. The potential for grain refinement provided by a method such as stirring with a transverse magnetic field where the effect is mainly on the arc and pool surface, will be decreased in this case. The effect of heat flow as a function of plate thickness may be a critical factor in grain refinement since it is possible that the length of the supercooled region in the weld pool will be affected by heat flow patterns dictated by plate thickness.

CONCLUSIONS

1. Electromagnetic stirring using a transverse field alters the weld pool shape but does not refine the columnar grain size of thick section, 30 mm, Ti-6Al-4V. The small supercooled region limits dendrite length, making grain refinement by tip fragmentation or secondary arm separation improbable.
2. There is minimal superheat in the weld pool 8 mm behind the centerline of the electrode. With the introduction of a rotating transverse magnetic field the weld pool temperature decreases and thermal gradients in the semi-solid zone also decrease.

3. Calculations based on constitutional supercooling and measured thermal gradients indicate cellular or dendritic growth of the advancing solid-liquid weld pool interface.

ON-GOING WORK

Based on the results presented herein work is continuing in the following areas.

1. The effect of heat flow on weld metal grain orientation and resulting grain size, shape and substructure must be established for unstirred and electromagnetically agitated weld pools. This work is being performed by comparing results of metallography of welds made on thin and thick section material.

2. The mode of solidification of titanium weld metal must be established and resulting changes due to a superimposed magnetic field observed. Removal of the liquid from the advancing liquid-solid interface by a technique known as impulse decanting will be employed in order to directly observe the mode of solidification and compare the results with the predicted growth.

3. A large separation of the solidus-liquidus in an alloy system encourages dendritic growth and this mode of solidification is essential for refinement due to dendrite tip fragmentation or secondary dendrite arm separation. Other alloy systems having large semi-solid zones will be investigated to enhance the understanding of the grain refinement mechanism as it applies to the titanium-aluminum system.

ACKNOWLEDGEMENT

The work presented in this paper was sponsored by the Office of Naval Research, Contract numbers N0014WR30087, NR 031-858 and N0014WR30088, NR 031-858.

REFERENCES

1. Brown, D. C., et al., "The Effect of Electromagnetic Stirring and Mechanical Vibration on Arc Welds," Welding Journal, June 1962, pp 241S-250S.

2. Simpson, R. P., "Controlled Weld-Pool Solidification Structure and Resultant Properties with Yttrium Inoculation of Ti-6Al-6V-2Sn Welds," Welding Journal, March 1977, pp 67S-77S.

3. Boldyrev, A. M., "The Effect of Methods of Weld Pool Modification on the Mechanical and Corrosion Properties of Welded Joints in Titanium Alloy OT4-1," Welding Production, 1979, No. 6, pp 5-8.

4. Garland, J. G., "Weld Pool Solidification Control," Metal Construction and British Welding Journal, April 1974, pp 121-127.

5. Private communication with M. E. Wells, DTNSRDC Code 2815.

6. Chernysh, V. P., et al., "Variation in the Temperature State of the Weld Pool during Electromagnetic Stirring," Automatic Welding, 1976, No. 7, pp 5-8.

7. Chernysh, V. P., and V. A. Pakharenko, "The Kinetics of Solidification of Pool Metal in Welding with Electromagnetic Stirring," Automatic Welding, 1979, No. 3, pp 29-30.

8. Abralov, M. A., and R. U. Abdurakhmanov, "Mechanism by which Electromagnetic Action Breaks Down Primary Structure of Weld Metal," Automatic Welding, 1982, No. 2, pp 14-17.

9. Pearce, B. P. and H. W. Kerr, "Grain Refinement in Magnetically Stirred GTA Welds of Aluminum Alloys," Metallurgical Transactions B, Vol. 12B, September 1981, pp 479-485.

10. Matsuda, F., et al., "Effect of Electromagnetic Stirring on the Weld Solidification Structure of Aluminum Alloys," Arc Physics and Weld Pool

Behaviour, The Welding Institute, Vol. 1, 1980.

11. Morgan-Warren, E. J., "Weld Metal Solidification and Its Control by Stirring," Arc Physics and Weld Pool Behaviour, The Welding Institute, Vol. 1, 1980.

12. Shelenkov, G. M., et al., "The Effect of Electromagnetic Stirring on the Properties of Welded Joints in Thin Titanium Sheets," Welding Production, 1974, No. 12, pp 34-37.

13. Shelenkov, G. M., et al., "The Effect of Electromagnetic Stirring on the Properties of Welded Joints in Titanium Alloy AT3," Welding Production, 1979, No. 2, pp 23-26.

14. Tiller, W. A., et al., Acta Metallurgica, Vol. 1, 1953, p 428.

15. Chalmers, B., Principles of Solidification, John Wiley and Sons, Inc., New York, 1964.

16. Heiple, C. R. et al., "Surface Active Element Effects on the Shape of GTA, Laser, and Electron Beam Welds," Welding Journal, Vol. 62, No. 3, pp 72-S 77-S.

17. Wagner, C., "Theoretical Analysis of Diffusion of Solutes During the Solidification of Alloys," Journal of Metals, February 1954, pp 154-160.

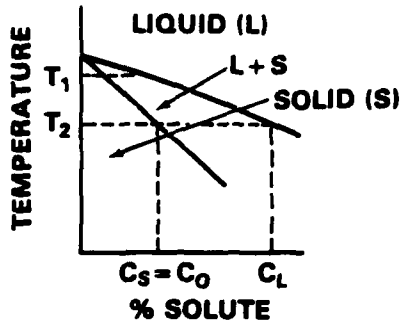

1a. EQUILIBRIUM COMPOSITIONS OF SOLID AND LIQUID

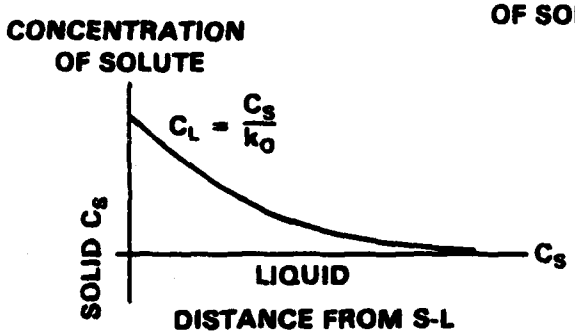

1b. DISTRIBUTION OF SOLUTE IN LIQUID

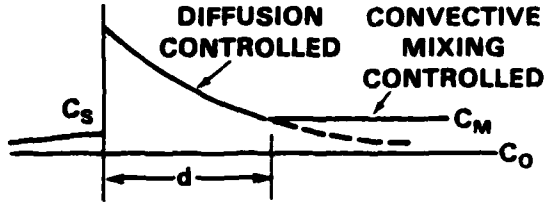

1c. DISTRIBUTION OF SOLUTE WITH MIXING OF LIQUID

1d. LIQUIDUS TEMPERATURE AS A FUNCTION OF DISTANCE (ACCORDING TO SOLUTE DISTRIBUTION IN 1b.)

1e. LIQUIDUS TEMPERATURE AS A FUNCTION OF DISTANCE (ACCORDING TO SOLUTE DISTRIBUTION IN 1c.)

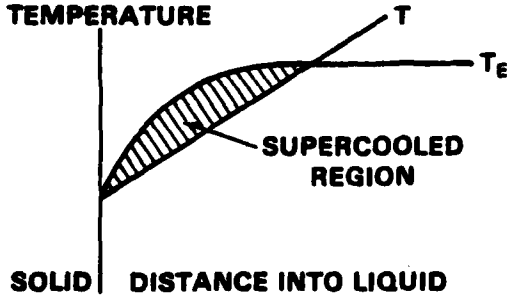

1f. CONSTITUTIONAL SUPERCOOLING

Figure 1 - Effects of Solute Redistribution on the Liquid Alloy

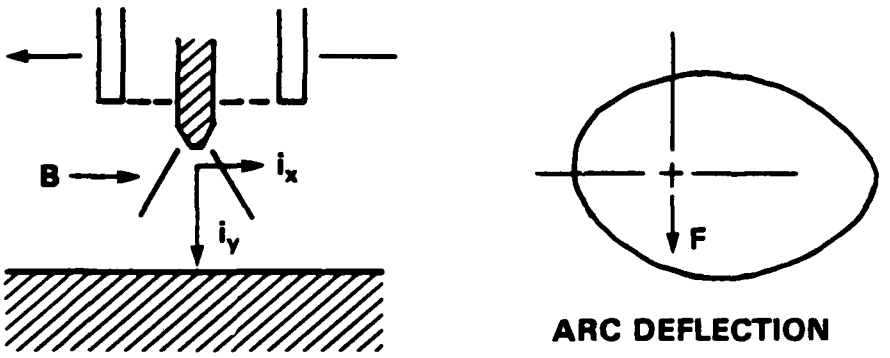

2a. TRANSVERSE MAGNETIC FIELD

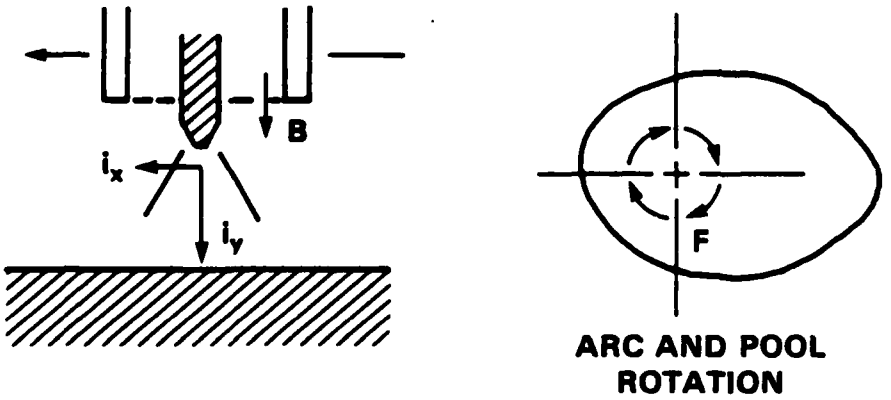

2b. LONGITUDINAL MAGNETIC FIELD

Figure 2 - Resultant Forces on Arc due to Superimposed Magnetic Field

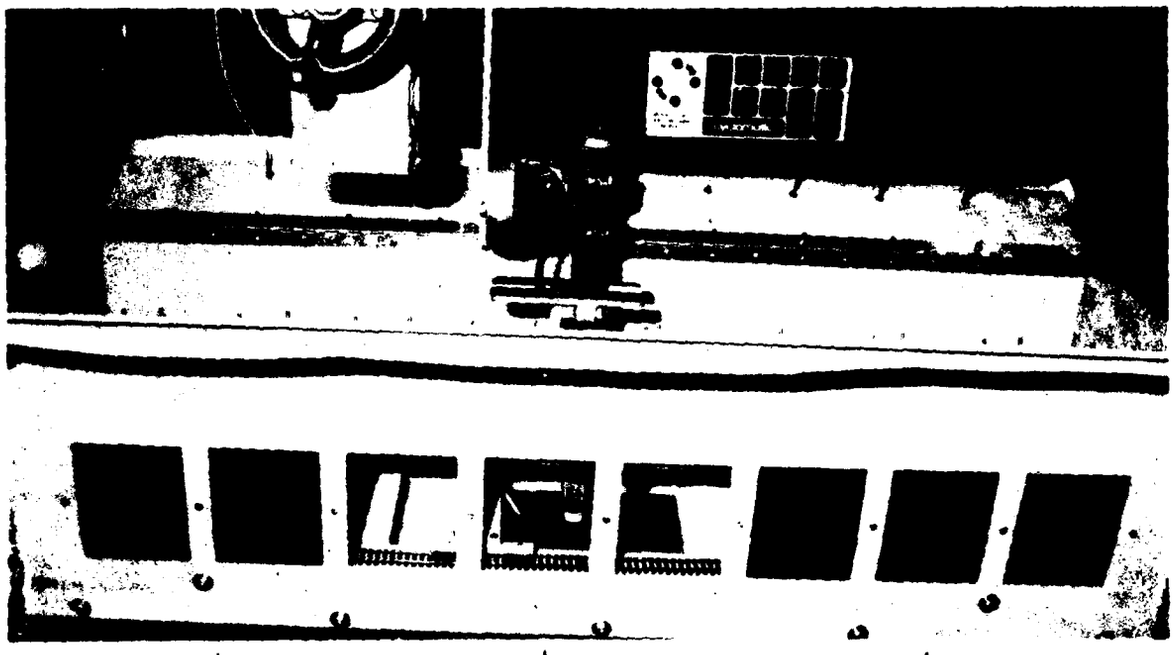

(a) OVERALL VIEW

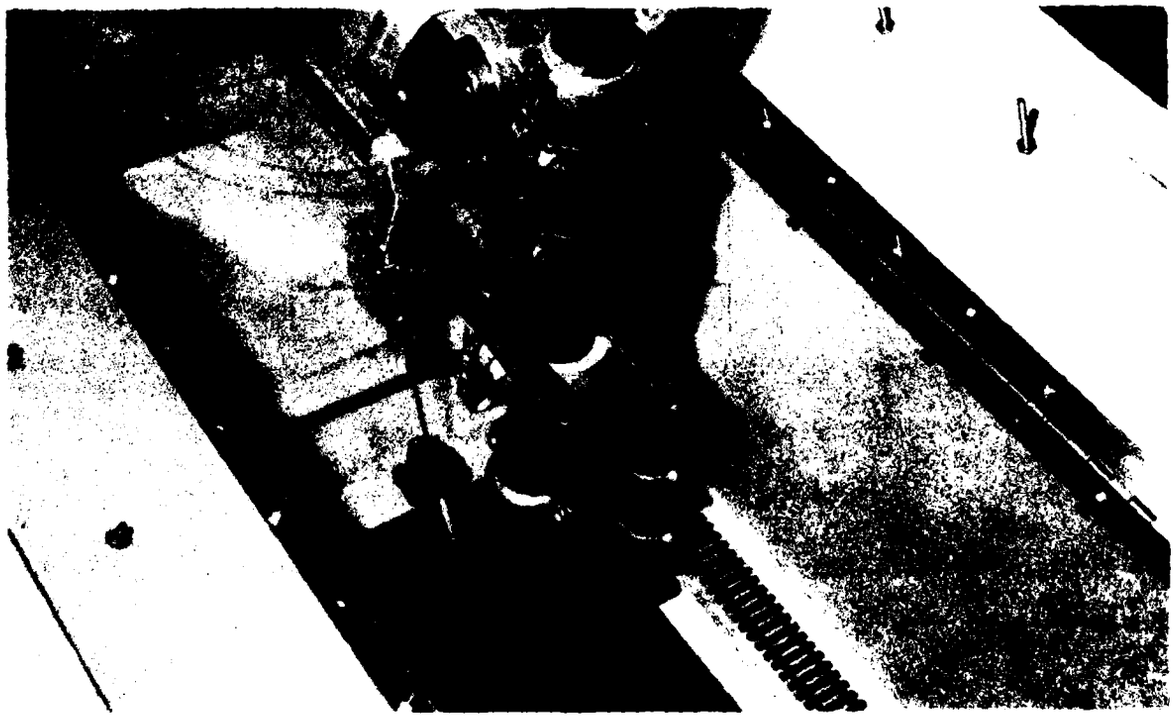

(b) CLOSE-UP VIEW OF THERMOCOUPLE AND CARRIAGE

Figure 3 - Weld Temperature Profiling Equipment

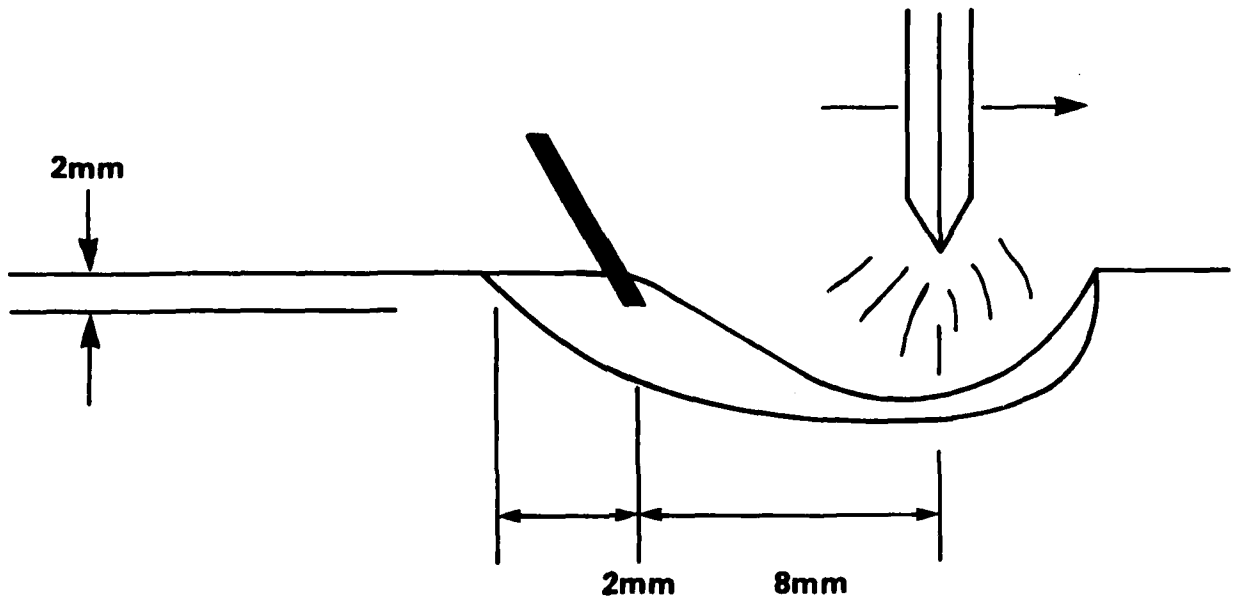

Figure 4 - Position of Thermocouple in Weld Pool

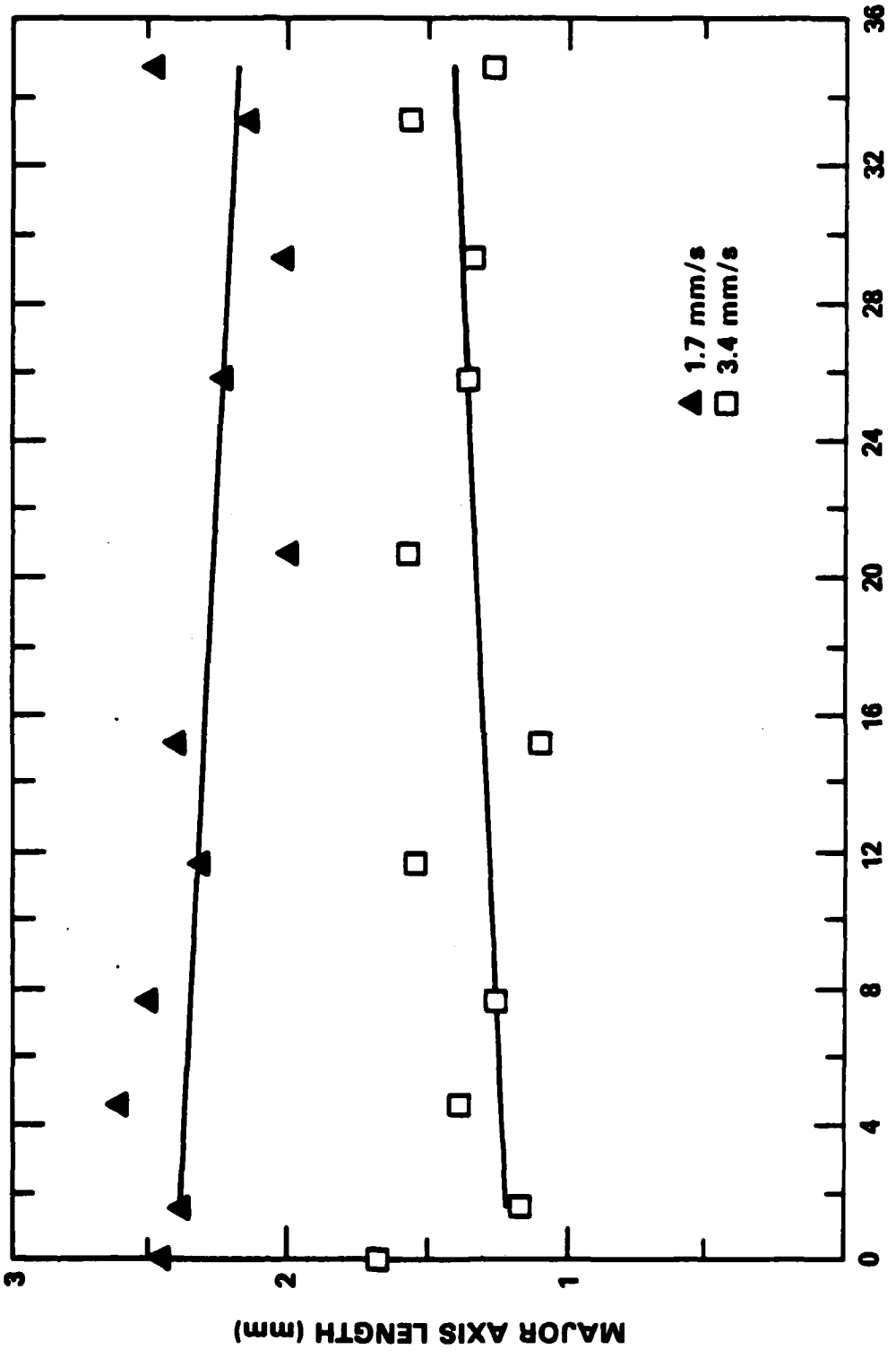

Figure 5 - Effect of Frequency of Arc Rotation on Columnar Grain Length

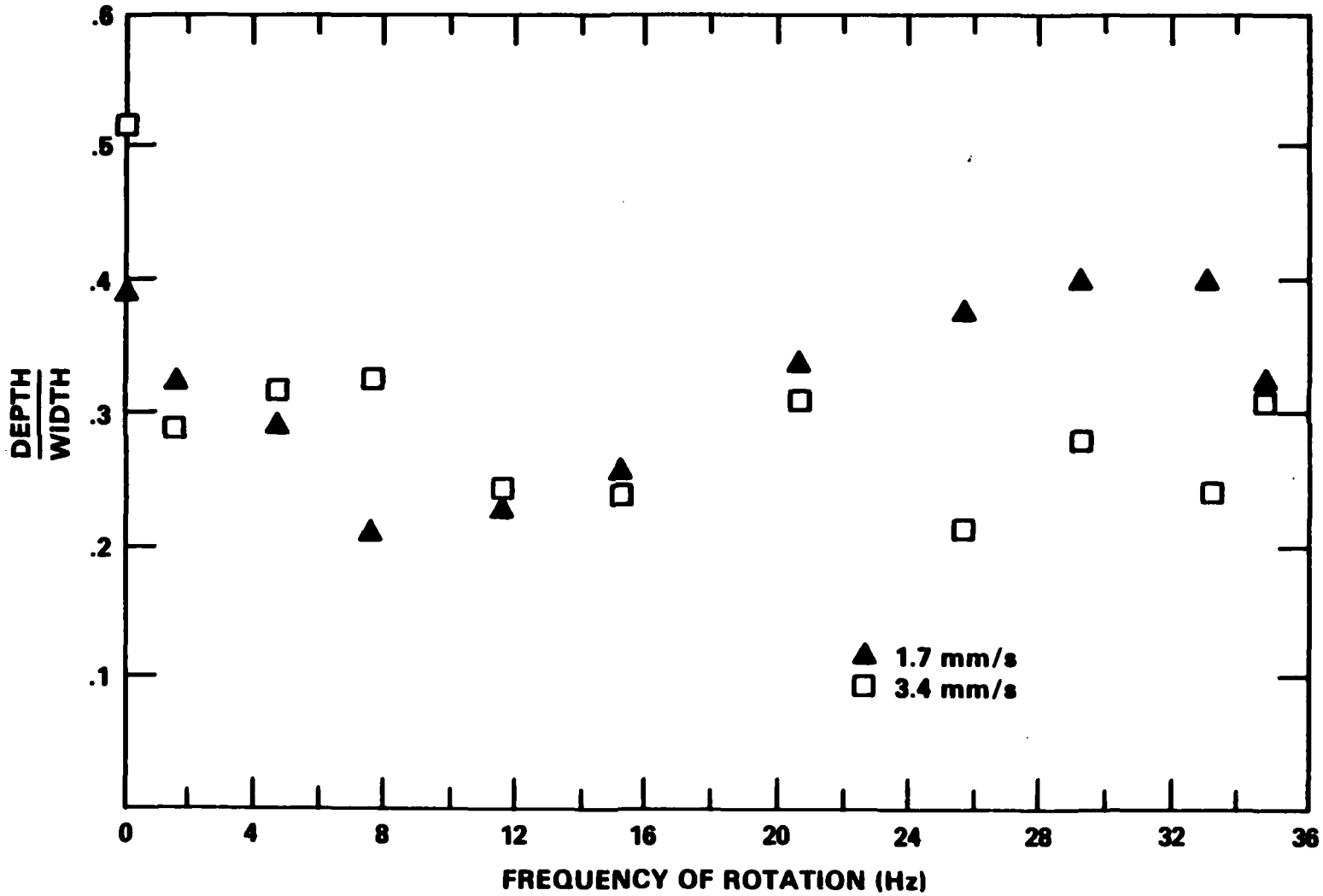

Figure 6 - Effect of Frequency of Arc Rotation on Bead Shape

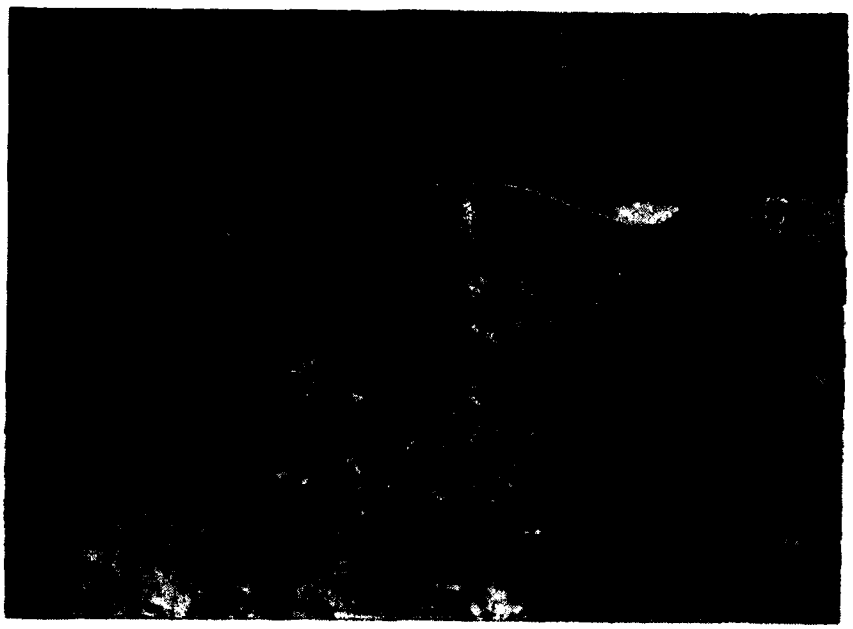

1 cm

CONTROL

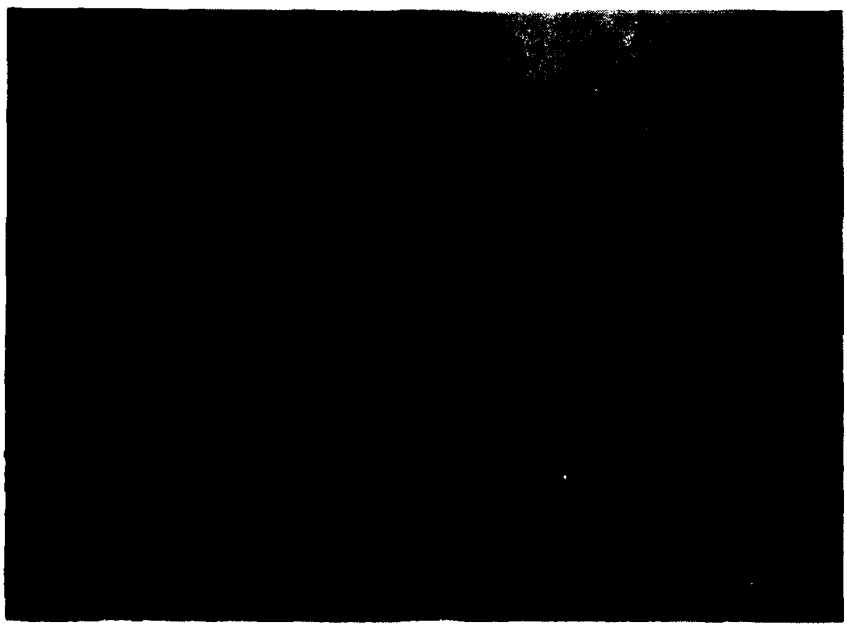

1 cm

FREQUENCY OF ROTATION 7.5 HZ

Figure 7 - Effect of Stirring on Columnar Grain Size

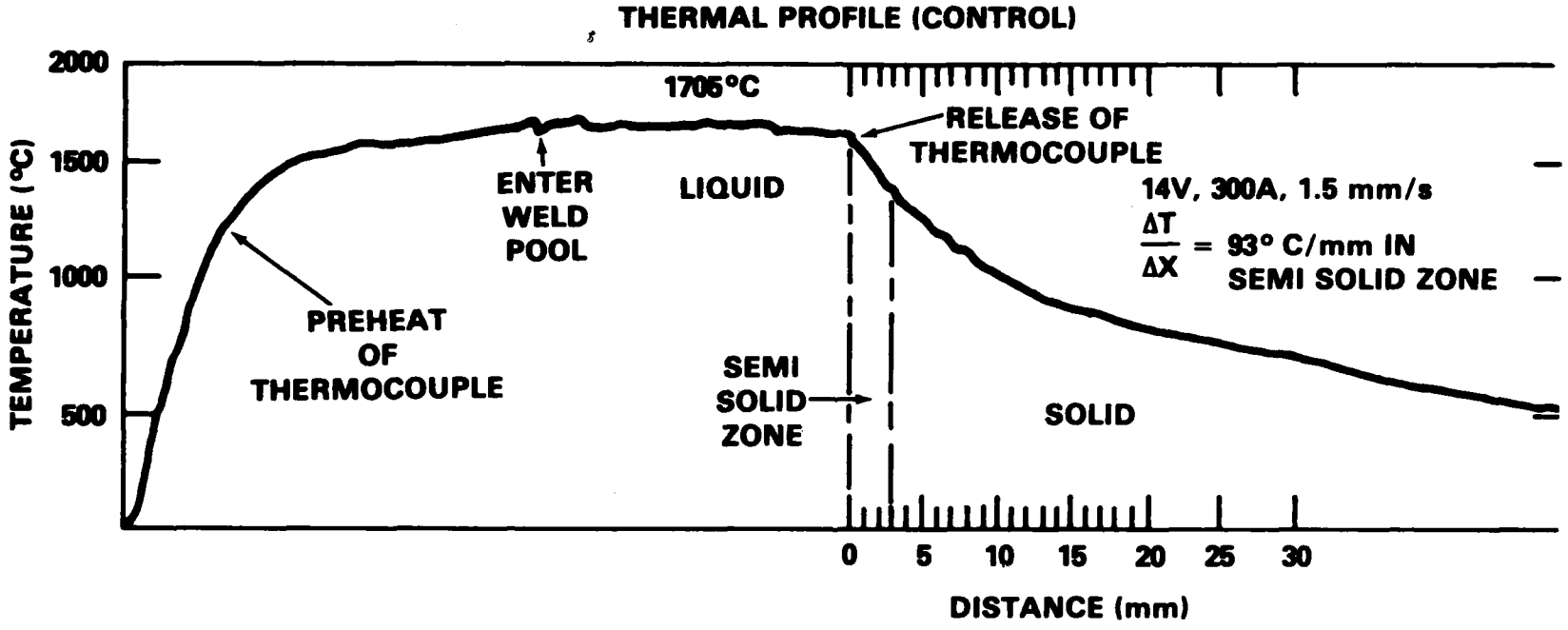

Figure 8 - Thermal Profile of Unstirred Specimen

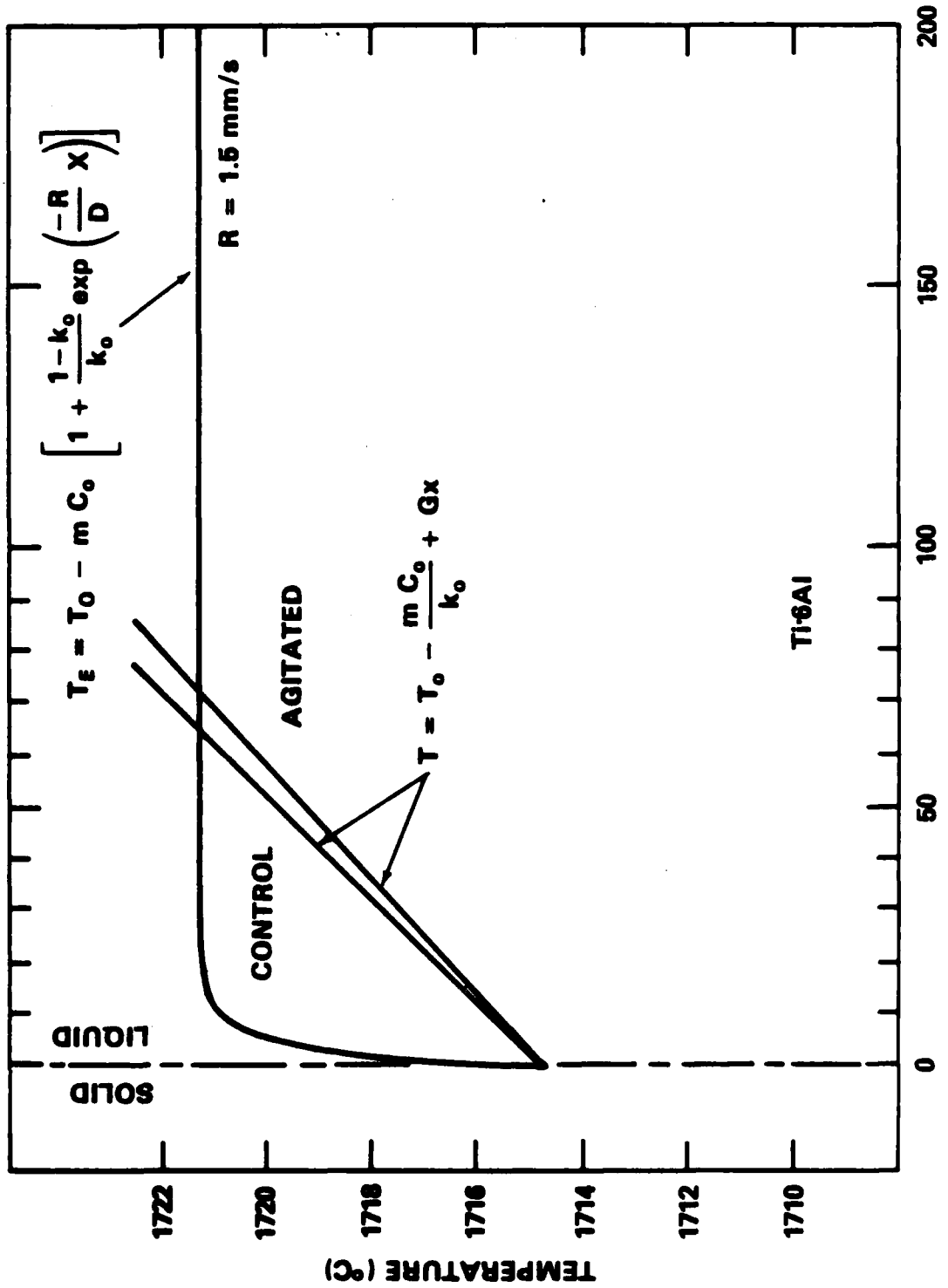

Figure 9 - Liquidus Temperature and Weld Pool Thermal Gradients

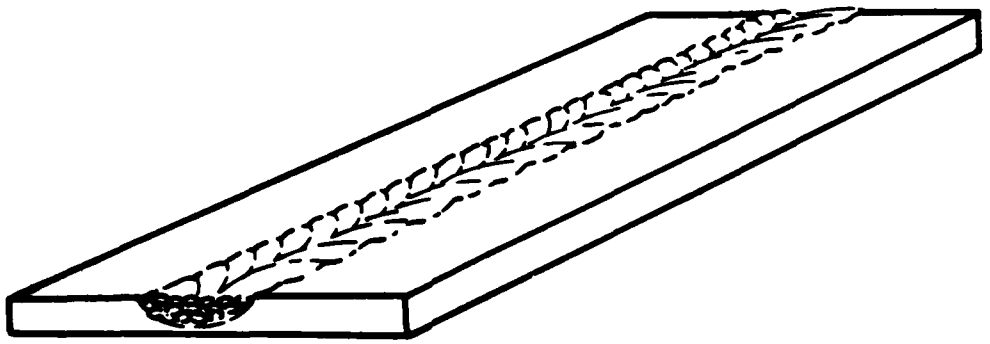

(a) THIN PLATE
2-D HEAT FLOW

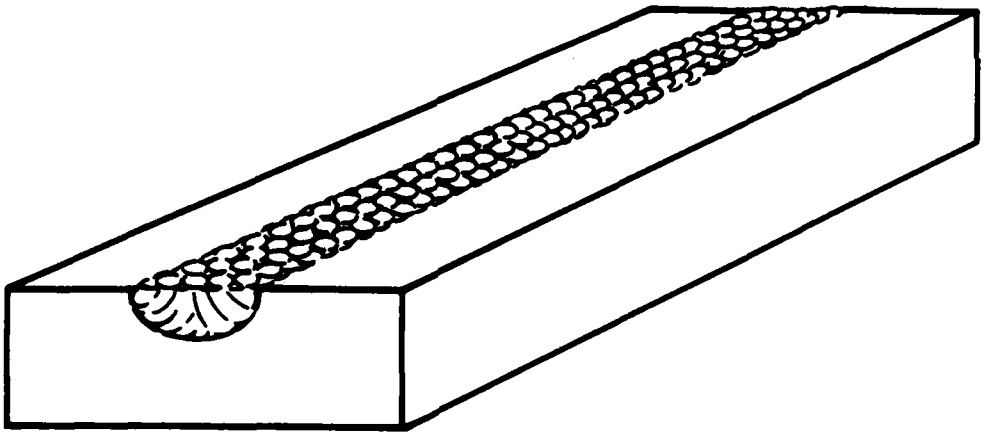

(b) THICK PLATE
3-D HEAT FLOW

Figure 10 - Schematic Grain Orientation

INITIAL DISTRIBUTION

Copies	Center Distribution	
1 ONR 431	Copies	Code
2 NAVSEA	1	1720.1
1 SEA 05M2	1	012
1 SEA 05R25	1	012.3
2 NRL	1	2801
Code 6300 Rath	1	2803
Code 6300 Judy	1	2809
1 Colorado School of Mines Golden, Colorado 80401 Attn: Professor G. R. Edwards	5	281
	2	2811
1 Massachusetts Institute of Technology Materials Processing Center Cambridge, Massachuseets 02139 Attn: Professor T. W. Eager	10	2815
	1	522.1
1 Oak Ridge National Laboratory Oak Ridge, Tennessee 37830 Attn: Dr. S. A. David		
1 U. S. Naval Academy Annapolis, MD 21402 Attn: Professor D. F. Hasson		
1 Betis Atomic Power Lab ZAP 14B P.O. Box 79 West Mifflin, PA 15122 Attn: Mr. B. Hyatt		
12 DTIC		

DTNSRDC ISSUES THREE TYPES OF REPORTS

1. DTNSRDC REPORTS, A FORMAL SERIES, CONTAIN INFORMATION OF PERMANENT TECHNICAL VALUE. THEY CARRY A CONSECUTIVE NUMERICAL IDENTIFICATION REGARDLESS OF THEIR CLASSIFICATION OR THE ORIGINATING DEPARTMENT.

2. DEPARTMENTAL REPORTS, A SEMIFORMAL SERIES, CONTAIN INFORMATION OF A PRELIMINARY, TEMPORARY, OR PROPRIETARY NATURE OR OF LIMITED INTEREST OR SIGNIFICANCE. THEY CARRY A DEPARTMENTAL ALPHANUMERICAL IDENTIFICATION.

3. TECHNICAL MEMORANDA, AN INFORMAL SERIES, CONTAIN TECHNICAL DOCUMENTATION OF LIMITED USE AND INTEREST. THEY ARE PRIMARILY WORKING PAPERS INTENDED FOR INTERNAL USE. THEY CARRY AN IDENTIFYING NUMBER WHICH INDICATES THEIR TYPE AND THE NUMERICAL CODE OF THE ORIGINATING DEPARTMENT. ANY DISTRIBUTION OUTSIDE DTNSRDC MUST BE APPROVED BY THE HEAD OF THE ORIGINATING DEPARTMENT ON A CASE-BY-CASE BASIS.

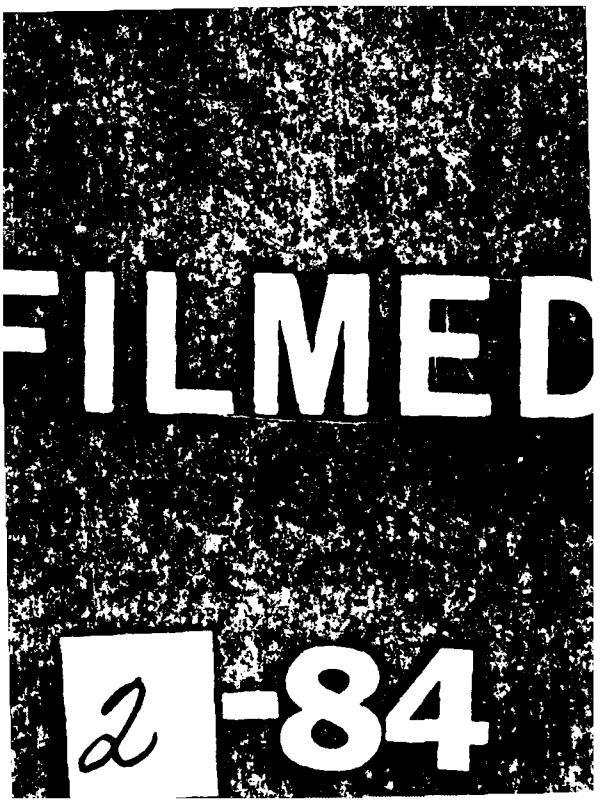
FILMED
2-84